NUCET NUCLEAR ENERGY AND TECHNOLOGY

Nuclear Energy and Technology 11(1): 1–12
DOI 10.3897/nucet.11.130422

Research Article

Assessing the suitability of two-group cross-sections and diffusion coefficients derived from SERPENT-2 for small modular reactor ACP-100

Md. Abidur Rahman Ishraq[1], Anton Evgenivich Kruglikov[1]

1 *National Research Nuclear University MEPhI (Moscow Engineering and Physics Institute), Moscow, Russia*

Corresponding author: Md Abidur Ishraq (abidur.ishraq@gmail.com)

Academic editor: Zeyun Wu ♦ **Received** 24 June 2024 ♦ **Accepted** 9 December 2024 ♦ **Published** 14 February 2025

Citation: Ishraq MAR, Kruglikov AE (2025) Assessing the suitability of two-group cross-sections and diffusion coefficients derived from SERPENT-2 for small modular reactor ACP-100. Nuclear Energy and Technology 11(1): 1–12. https://doi.org/10.3897/nucet.11.130422

Abstract

The focus of this work is to analyse the suitability of two-group diffusion coefficients and macro constants generated from SERPENT using out-scattering approximation (OSA), transport correction (TRC) and cumulative migration methods (CMM) for fuel and non-fuel materials. For this purpose, various assembly and core models of ACP-100 SMR were designed. Assessment of these constants was conducted using COMSOL Multiphysics. For six distinct fuels, the best models were proposed with the least error margin in k_{eff}. Fuel material affects the group constants of non-fuel components except for radial reflectors. The sufficiency of two-group calculation was justified through spectrum analysis. Additional analysis revealed that MOX-RG has the hardest spectrum among all the fuels. Moreover, the effectiveness of boric acid to control excess reactivity was observed. Subcriticality was achieved for all fuel types except MOX-RG at a boric acid concentration of 4500 ppm. The influence of variation of boric acid concentrations on group constants was investigated using TRC and OSA. The reactivity difference between SERPENT and COMSOL was determined. It was found that OSA generates the most accurate results for MOX-RG with maximum 863 pcm error, while TRC produces higher accuracy with maximum error of approximately 250 pcm for other fuels.

Keywords

Two-group constants, Out-scattering approximation (OSA), Hydrogen transport correction (TRC), Cumulative migration methods (CMM), SERPENT, Partial differential equation (PDE)

Introduction

Monte Carlo (MC) method-based programs can be used to build complex and detailed models of nuclear reactors and to calculate various neutronic behaviour of the reactor. However, in recent times, there has been a growing interest in the utilization of Monte Carlo (MC) tools for the generation of multi-group cross-sections in deterministic reactor core calculations (Fridman and Leppänen 2011; Park et al. 2012). This increased interest can be attributed to the inherent flexible and easy modelling capabilities offered by Monte Carlo programs such as SERPENT. The primary intent of Serpent is expressly directed towards lattice physics applications, encompassing the precise generation of homogenized few-group constants used for the simulation of complete core behaviour in comprehensive core simulators (Leppänen 2013). These constants can be used as input parameters for programs to solve multi-group diffusion equations.

The neutron diffusion theory stands as a fundamental and extensively employed methodology for analysing the

spatial distribution of neutrons within a reactor. This approach offers the flexibility to characterize the neutron energy spectrum across various user-defined groups (Stacey 2018). The energy group definition is determined by the user based on the accuracy of calculation and the type of reactor. In the context of light water reactors, a two-group representation proves highly beneficial for expressing the neutron balance statement in practical implementation (Lee 2020). Two-group diffusion calculations are effective for conventional light water reactors (LWR) (Gürdal and Tombakoğlu 2009). However, It is necessary to evaluate whether the two-group diffusion equations can be applied to unconventional light water reactors (LWRs) like small modular reactors (SMRs) employing different fuels. In the present study, the spatially-dependent neutron diffusion equations, specifically the two-group formulation, were implemented using COMSOL Multiphysics 6.1 (COMSOL 2008) to model and simulate neutron transport within a three-dimensional representation of a light water-based small modular reactor ACP-100.

Making sense of different materials and their effects within a nuclear reactor core (cross section homogenization) is tough. This has mainly been done for large reactors, but lately, smaller ones are also getting this special attention in recent times (Fejt and Frybort 2018). In this regard, existing data library for conventional reactor may not be sufficient. For small sized reactor An existence of a general cross-section library would have a positive impact. To generate the diffusion coefficients and cross section SERPENT is getting popularity as it offers various methods of calculation (Fejt et al. 2022). The main problem of the small sized or small modular reactors is high neutron leakage rate, which shortens the validity of using diffusion theory (Vanyi et al. 2022). So, analysis of generating diffusion coefficients and applicability of diffusion theory in SMR is required.

Diffusion coefficients can be generated by many methods for different geometries using SERPENT (Zhong 2014). User-defined hydrogen transport correction (TRC) and cumulative migration method (CMM) are two methods to produce diffusion coefficients (Shchurovskaya et al. 2020). The so-called in-scattering approximation and out-scattering approximation are the default methods that SERPENT-2 provides to generate diffusion coefficients (Leppänen et al. 2016). The purpose of this study is to analyse which model/models produce diffusion coefficients and group constants with sufficient accuracy for different fuels to solve multi-group equations. Furthermore, an analysis has been conducted on the comparison of two-group constants and the eigenvalues derived from employing these constants. The investigation encompasses several fuels and employs diverse geometric models for both the fuel assembly and the core of the ACP-100 reactor.

Flux distribution analysis can be conducted to evaluate the validity of the codes (Snoj et al. 2011). The spatial flux distributions generated by both programs were compared and analyzed. Additionally, an energy-based neutron spectrum analysis was performed to support the implementation of a 2-group model.

Managing excess reactivity in begin of life (BOL) is one of the most important factors that plays a vital role in many safety and economic aspects of any power reactor (Galahom 2020; Galahom 2021). The most common method to control early excess reactivity of a pressurized water reactor (PWR) is to use soluble boric acid (H_3BO_3) as a chemical shim in the moderator (Fadaei 2011). The presence of ^{10}B in H_3BO_3 changes some of the group constants and diffusion coefficients (Wan et al. 2021). So, it is important to analyse the accuracy of the generation of group constants for various concentrations of H_3BO_3 for all the fuels. In the present work, this was also explored by using SERPENT following different methods.

Calculation method and model

Code and data library descriptions

SERPENT

To construct the simple 2D and 3D models of different fueled ACP-100 assemblies and design detailed core models in this research, the neutronic code SERPENT 2.1.32 was used. SERPENT is a continuous-energy three-dimensional Monte Carlo particle (neutron and photon) transport code, designed and upheld by the VTT Technical Research Centre of Finland since 2004. The original purpose of this code was to serve as a simplified neutron transport code for reactor physics simulations, it has evolved into a tool with diverse applications, encompassing group constant generation, coupled multi-physics scenarios, fusion neutronic, and radiation shielding (Leppänen et al. 2015). The complex neutronic computations were executed using cross-section data sourced from the nuclear data library ENDF/B-VII.0 (Chadwick et al. 2006).

COMSOL Multiphysics

The COMSOL software, functioning as a finite element-based multiphysics numerical analysis tool, boasts extensive applications in various realms of physics and engineering, accommodating coupled phenomena or multiphysics scenarios (COMSOL 2008). Characterized by an integrated user interface, it facilitates the direct input of coupled systems of partial differential equations (PDE). Moreover, the COMSOL application builder is instrumental in constructing specialized applications grounded in physics models. The adaptive mesh refinement feature enhances solution accuracy by strategically augmenting the number of elements in regions with the greatest numerical error, thereby mitigating spatial discretization errors in the obtained results. In this study, COMSOL Multiphysics 6.1 was used to solve the two-group diffusion equation of detailed cores with different fuels.

Core and assembly design specifications and description of the models

This research investigation delves into the generation of diffusion coefficients and two-group constants for both 2D and 3D models representing fuel assemblies and detailed core configurations of the Chinese Small Modular Reactor (SMR) known as ACP-100. This study encompasses six distinct fuel types, employing various methods to produce diffusion coefficients available in SERPENT. The objective is to identify the most appropriate constants for solving the two-group diffusion equation. The ACP-100 (Access Control Point-100), characterized by an innovative Pressurized Water Reactor (PWR) design, incorporates a passive safety system and integrated reactor design technology, anticipating an electrical power output within the range of 100–125 MWe (Zhong 2014; Ishraq et al. 2024b). The ACP-100 reactor core consists of 57 partial-height fuel assemblies (FAs), each housing 264 fuel elements. Table 1 presents the principal design and technical parameters of the reactor core employed in this research endeavour. The configurations of the fuel element and fuel rod adhere to the standards of a typical Pressurized Water Reactor (PWR) assembly. The study encompasses six distinct fuels, comprising three variations of UOX with different enrichment, homogeneous Th, and both Weapon and Reactor Grade (WG, RG) MOX. A detailed description of these fuels is available in Table 2, while comprehensive details regarding the considered core models are provided in Table 3 (Ishraq et al. 2024a). Fig. 1 offers visual depictions of a standard fuel pin and radial view of an assembly. The radial geometries of the cores are presented in Fig. 2.

Table 1. Technical parameters of the ACP-100 core (Song, 202; Ishraq et al. 2024b; Ishraq et al. 2024c)

Components	Parameters	Values
Core	Thermal power (MW_{th})	385
	Electrical power (MW_e)	100–125
	Coolant average temperature (K)	600
	Fuel average temperature (K)	1100
	Number of fuel assemblies	57
	Fuel (UO_2) density (g/cm^3)	10.97
	Coolant (light-water) density (g/cm^3)	0.6628
	Core/fuel active section height (m)	2.15
	Core radius (m)	1.183
	Core power density (MW/m^3)	68
Fuel assembly	Total number of rods	289 (17×17 square array)
	Number of fuel rods	264 (28 IFBAs)
	Number of control rods	20 + 5 GTs
	Fuel assembly pitch (cm)	21.504
Fuel element	Radius of the fuel rod (cm)	0.4095
	Radius of IFBA rods (cm)	0.4158
	Gap outer radius (cm)	0.4177
	Clad outer radius (cm)	0.475
	Rod pitch (cm)	1.26
	Gap material	O_2 gas
	Clad material	Zircaloy-2

Additionally, Fig. 3 illustrates the axial geometric views of both 2D. 3D mesh model of the core built in COMSOL Multiphysics is shown in Fig. 4.

The main design/technical parameters of the reactor core utilized in this research work are presented in Table 1.

Methodology and work flow sequence

In this study, 2D and 3D models of Fuel Assemblies (FAs) were constructed and detailed core models were developed for six distinct fuel configurations using SERPENT. To obtain essential two-group constants and diffusion coefficients, three distinct approaches were employed: the Out-Scattering Approximation (OSA), the Cumulative Migration Method (CMM), and the Hydrogen Transport

Table 2. Description of the core models

Core Model ID	Description
Core Model 1	57 FAs with 3.0 wt.% enriched fuel
Core Model 2	57 FAs with 4.0 wt.% enriched fuel
Core Model 3	57 FAs with 4.45 wt.% enriched fuel
Core Model 4	57 FAs with Th fuel
Core Model 5	21 FAs with 16% Reactor Grade MOX 36 FAs with 4.45 wt.% enriched UOX fuel
Core Model 6	21 FAs with 2.65% Weapon Grade MOX 36 FAs with 4.45 wt.% enriched UOX fuel

Table 3. Isotopic composition of different fuels

Fuel	Nuclide	Composition (wt. %)	Density (g/cc)
UOX 3.0 wt. %	^{235}U	2.644	10.422
	^{238}U	85.503	
	^{16}O	11.853	
UOX 4.0 wt. %	^{235}U	3.526	10.424
	^{238}U	84.621	
	^{16}O	11.853	
UOX 4.45 wt. %	^{235}U	3.923	10.425
	^{238}U	84.224	
	^{16}O	11.853	
Th	^{232}Th	8.788	11.882
	^{235}U	3.919	
	^{238}U	75.411	
	^{16}O	11.882	
MOX-RG	^{238}Pu	0.282	10.36
	^{239}Pu	7.475	
	^{240}Pu	3.385	
	^{241}Pu	2.116	
	^{242}Pu	0.846	
	^{235}U	0.148	
	^{238}U	73.849	
	^{16}O	11.898	
MOX-WG	^{238}Pu	0.000	10.36
	^{239}Pu	2.477	
	^{240}Pu	0.156	
	^{241}Pu	0.01106	
	^{242}Pu	0.0026	
	^{235}U	0.171	
	^{238}U	85.335	
	^{16}O	11.752	

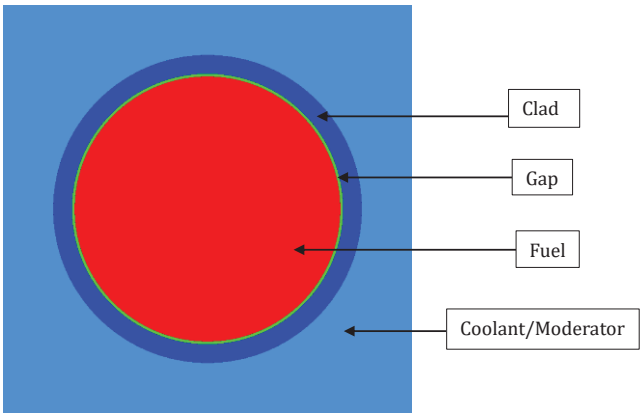

(a) Representative fuel pin/element

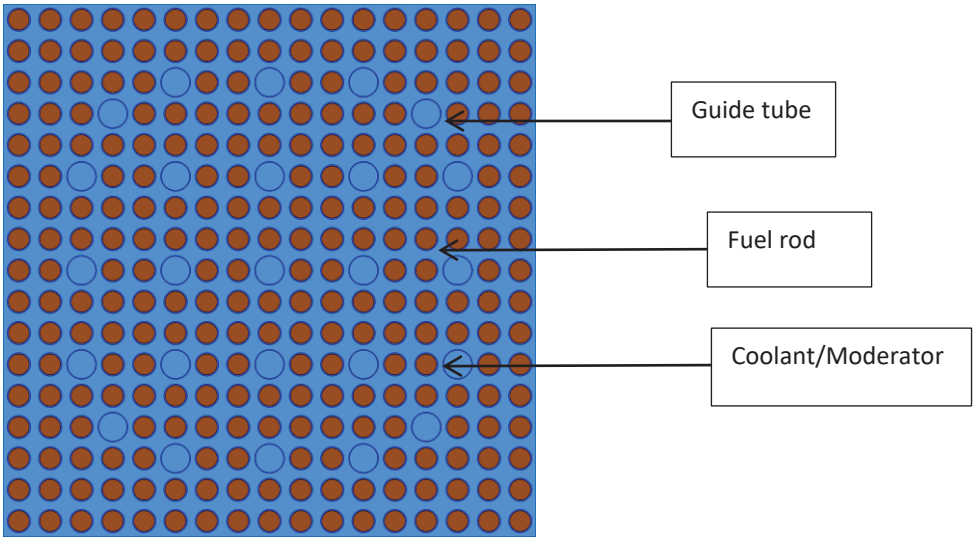

(b) Fuel assembly without IFBA rods

Figure 1. Diagrams of a typical fuel element and a fuel assembly. (**a**) Representative fuel pin/element. (**b**) Fuel assembly.

Correction Method (TRC). The history of 50,000 neutrons were tracked for 3000 cycles/batches (the first 200 of which were skipped) with reflective boundary conditions for assembly models and vacuum boundary conditions for core models in this study. The constants derived from these approaches served as the input parameters for solving the two-group diffusion equation for the core model. The numerical simulations were then conducted within the framework of COMSOL Multiphysics, which allowed for the determination of the eigenvalue, specifically the effective multiplication factor (k_{eff}). To support the validation of using the two codes a comparative analysis of spatial (Radial) flux distribution was presented for the fuel with 4.45% enrichment. To get higher statistical accuracy in SERPENT and produce more accurate group constants 50,000 neutron population with 5,00,000 cycles (first 200 were skipped) was used.

The impacts of various fuels and soluble boric acid on diffusion coefficients and two-group constants were also investigated. The analysis involved the construction of a 315-energy group spectrum for diverse fueled cores, considering various zones within the core. Soluble boric acid (H_3BO_3) is a very important chemical compound to control excess reactivity. So, the effect of H_3BO_3 for six distinct fuels and their group constants in the reflector zones using TRC and OSA methods were observed. The sequential methodological approach utilized in this study to obtain the desired results is visually represented in Fig. 5 as a flowchart. Table 4 outlines diverse models employed for the generation of diffusion coefficients and group constants within the SERPENT framework. Subsequently, these parameters were utilized as input in COMSOL Multiphysics for the solution of Partial Differential Equations (PDEs). In this study assembly discontinuity factor (ADF) was not considered. The two-group diffusion equations, that were used in this study are shown bellow (Stacey 2018):

$$-\nabla \cdot \mathrm{D}^1 \nabla \Phi_1(\vec{\mathbf{r}}) + \left(\Sigma_a^1 + \sum_s^{1\to 2}\right) \Phi_1(\vec{\mathbf{r}}) = \frac{1}{k}\left(v_1 \Sigma_f^1 \Phi_1(\vec{\mathbf{r}}) + v_2 \Sigma_f^2 \Phi_2(\vec{\mathbf{r}})\right) \quad (1)$$

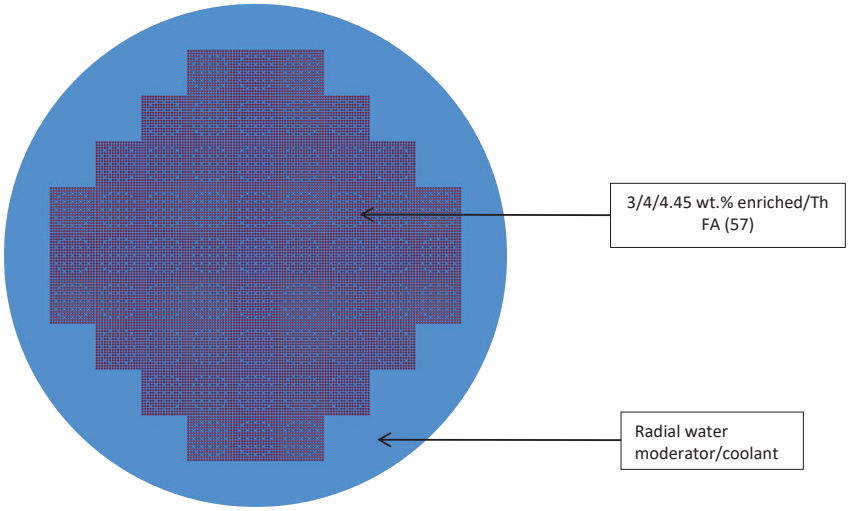

(a) Models 1, 2, 3 and 4

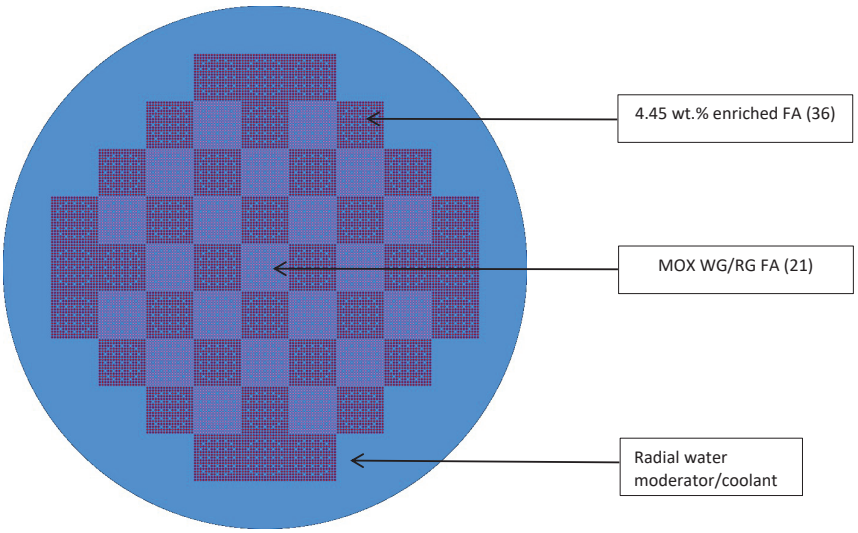

(b) Model 5 and 6

Figure 2. Radial view of the considered core models. (**a**) Models 1, 2, 3 and 4. (**b**) Models 5 and 6.

$$-\nabla \cdot \mathrm{D}^2 \nabla \Phi_2(\vec{\mathbf{r}}) + \sum_{a}^{2} \Phi_2(\vec{\mathbf{r}}) = \sum_{s}^{1} \rightarrow 2\Phi_1(\vec{\mathbf{r}}) \quad (2)$$

where D^1 and D^2 are diffusion coefficients, Σ_a^1 and Σ_a^2 are absorption cross-sections, Σ_f^1 and Σ_f^2 are fission cross-sections, υ_1 and υ_2 are average neutron yield, $\Phi_1(\vec{\mathbf{r}})$ and $\Phi_2(\vec{\mathbf{r}})$ are neutron flux for energy group 1 and 2 respectively, $\Sigma_S^{1\rightarrow 2}$ is scattering cross-sections from energy group 1 to 2. Default two-energy-group structure of SERPENT was used in this study which is separated at 0.625eV (Leppänen et al. 2015).

Description about the calculative methods of diffusion coefficients

Cumulative Migration Method (CMM)

The Cumulative Migration Method (CMM) offers a rigorous approach for calculating diffusion coefficients and transport cross sections in nuclear reactors. It leverages the concept of "migration area," which relates to the average squared distance a neutron travels before absorption. By employing one-group diffusion theory, CMM establishes a connection between migration area and the neutron's average squared flight length . This relationship is then extended to multi-group problems through the introduction of "cumulative groups." These groups encompass energy ranges from the top energy level down to a specific group boundary. CMM calculates "cumulative migration areas" for these groups and utilizes them, along with average squared flight lengths obtained from Monte Carlo simulations, to derive group-wise diffusion coefficients. This method provides a more accurate and efficient way to characterize neutron transport within complex reactor lattices (Liu et al. 2018).

Out-Scattering approximation (OSA)

The out-scatter approximation (OSA) simplifies the treatment of neutron scattering within reactor physics calculations. This approach assumes that the linearly anisotropic component of the scattering matrix, which describes the angular dependence of scattering events, has negligible

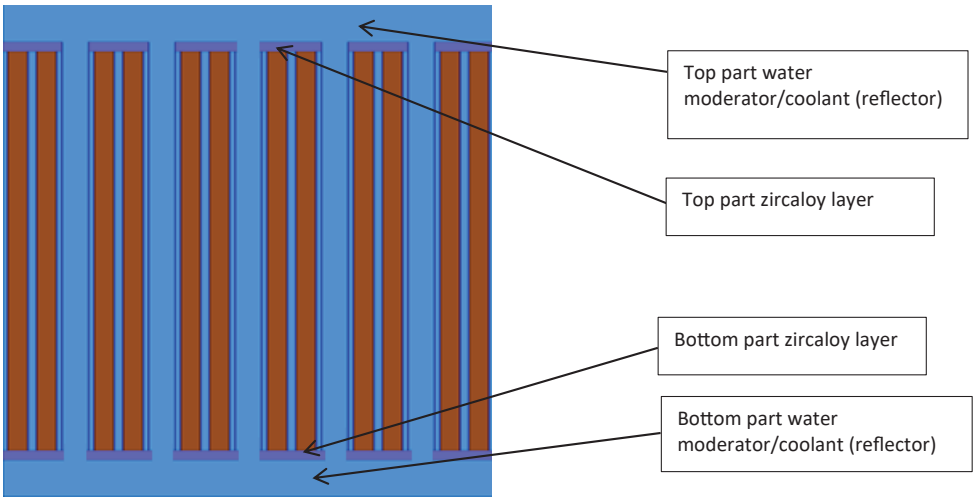

Figure 3. Axial view of the 3D FA model.

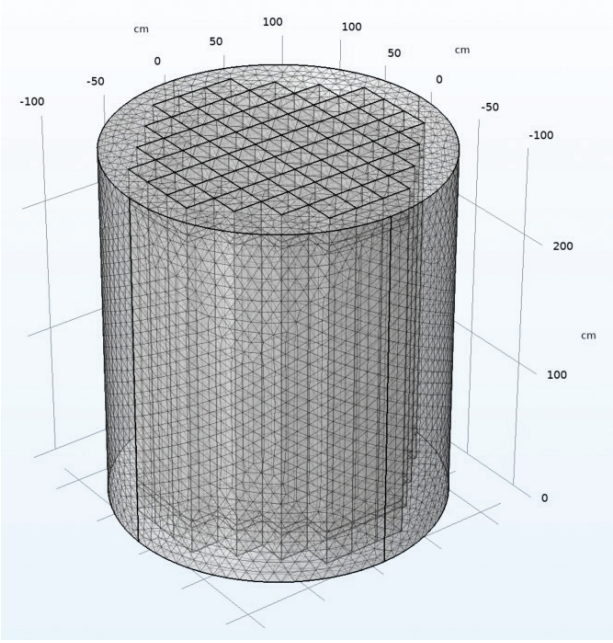

Figure 4. 3D mesh model of the core modeled in COMSOL.

impact on energy transfer between neutrons and nuclei. Due to its relative ease of implementation, this approximation is employed in various lattice physics codes, including SERPENT 2 (Ványi et al. 2021). The validity of this assumption is generally accepted when two conditions are met: 1) weak absorption within the medium, and 2) minimal significance of anisotropic scattering (Stammler and Abbate 1983).

Transport Correction Approximation (TRC)

Transport Correction Approximation (TRC) address a limitation of the out-scatter approximation in neutron transport calculations. This approximation assumes minimal influence of scattering angles on energy transfer, simplifying calculations. TRC, introduced by the Neutron Leakage Conservation (NLC) method (Herman et al. 2013), improve accuracy. NLC defines a simplified geometry (like a slab of pure hydrogen) where diffusion theory is considered valid. By comparing diffusion theory results with a Monte Carlo transport simulation (SERPENT) for this geometry, the NLC method calculates TRC for each energy group. The TRC values basically show how much the two methods (diffusion theory and Monte Carlo simulation) differ in their predictions about neutron behavior. Finally, applying these TRC to transport cross-sections refines their accuracy in representing neutron behavior within real reactor lattices (Vanyi et al. 2022).

Results and discussion

Effective multiplication factor (k_{eff})

Effective multiplication factor k_{eff} serves as a quantitative measure, representing the criticality state of the system. Within Table 5, a comparative analysis is presented, comparing the k_{eff} values derived from SERPENT and COMSOL Multiphysics using two-group constants obtained from diverse models of fuel assemblies, each representative of distinct fuel compositions generated from SERPENT. The statistical uncertainty associated with the k_{eff} values calculated using SERPENT was less than 3 pcm for all fuel types. For UOX-based fuel, models 2, 3, 4 show close results, while the deviations from the Monte Carlo calculation in these models are the smallest. For options with weapons-grade and reactor-grade plutonium, a higher deviation is observed, but still not exceeding 0.4%, which can be considered a good result. The higher deviation can be explained by the fact that a larger proportion of fissile nuclide is present in the fuel elements with Pu, which creates higher non-uniformity throughout the fuel assembly. This can also explain the better agreement between the results when using the CMM method to calculate the diffusion coefficient, this is especially evident for weapons-grade plutonium.e multiplication factor, denoted as k_{eff}, is precisely defined as the quantitative relationship between the number of neutrons generated from fission events within each succeeding generation and the corresponding amount of neutrons absorbed in the antecedent generation, within the context of a finite medium.

Table 4. Description of different sets of constants

Model	Fuel		Radial water		Top/bottom part water		Top/bottom part Zircaloy layer	
	D_i	Σ_i	D_i	Σ_i	D_i	Σ_i	D_i	Σ_i
1	3d FA OSA	3d FA	3d core OSA	3d core	3d FA OSA	3d FA	3d FA OSA	3d FA
2	3d FA OSA	3d FA	3d core TRC	3d core	3d FA OSA	3d FA	3d FA OSA	3d FA
3	3d FA OSA	3d FA	3d core TRC	3d core	3d FA TRC	3d FA	3d FA OSA	3d FA
4	2d FA OSA	2d FA	3d core TRC	3d core	3d FA OSA	3d FA	3d FA OSA	3d FA
5	2d FA OSA	2d FA	3d core TRC	3d core	3d FA TRC	3d FA	3d FA OSA	3d FA
6	2d FA CMM	2d FA	3d core TRC	3d core	3d FA TRC	3d FA	3d FA OSA	3d FA

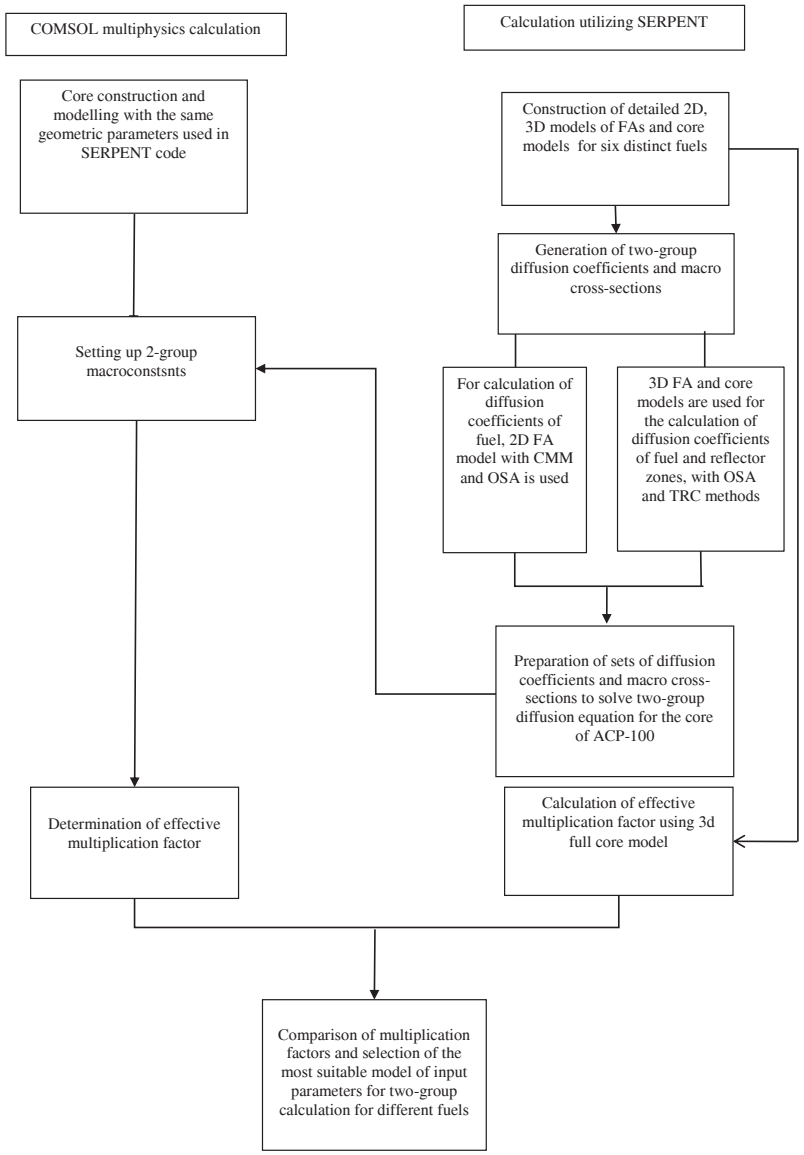

Figure 5. Flow chart describing the sequence of steps followed in the analysis.

Two group diffusion coefficients and macroscopic cross-section

Two-group diffusion coefficients and macroscopic cross-sections for fuel and non-fuel materials were computed across various configurations of detailed cores containing different fuel materials. The diffusion coefficients were determined through the application of both the Out-scattering Approximation (OSA) and the Transport Correction Method (TRC) for non-fuel components. For fuel materials, only the default OSA method was used. For all the fuel types, the effective delayed neutron fraction (β_{eff}), which is an important safety parameter was calculated. The outcomes of these calculations are delineated in Tables 6–9. It is found that fuel materials do not affect the constants of radial water. So, for different fuels, it is not necessary to prepare constants for them. However, variations of fuels have noticeable effects on top and bottom reflectors and Zircaloy layers. Hence, these constants must be prepared in case of different fuels. Additionally, it is noteworthy that none of the constants exhibit significant variations across differently enriched UOX fuel compositions.

Spatial flux distribution

The radial distributions of thermal and fast neutron fluxes were analyzed and compared between the two programs. The results are presented in Fig. 6. Fig. 6(a) illustrates the thermal flux distribution across half of the active zone. A noticeable increase in neutron population can be observed at the fuel zone boundary, primarily attributed to the radial reflector's neutron moderating properties. The maximum relative error in thermal flux between the two programs was approximately 10%. Fig. 6(b) depicts the radial flux distribution of fast neutrons, with a maximum relative error of around 3%.

Energy-dependent neutron flux spectrum

The neutron flux spectrum within a nuclear reactor determines the distribution of neutron energies, exerting a direct influence on fission, capture, and scattering reactions, as well as critical reactor parameters such as reactivity and power density. Fig. 7 illustrates the normalized neutron flux per unit lethargy for designed core models at the inception of their operational life (BOL), featuring various fuels. To achieve this, the SERPENT code utilized a predefined group structure known as "Tripoli 315-group structure" (Zheng et al. 1998). It can be observed that no strong resonance is found in the thermal energy zones. So for thermal reactors, the two-group approximation can produce results with sufficient accuracy. 3% UOX fuel has the softest neutron energy spectrum whereas MOX-RG has the hardest spectrum. For thermal neutrons, the absorption cross-sections for ^{238}U, ^{235}U and ^{239}Pu are 2.68, 99 and 270 barn respectively obtained from JANIS 4.0 (Lamarsh and Baratta 2001; Soppera et al. 2014). With the increase in enrichment, the fraction of ^{235}U with higher absorption cross-section increases which hardens the neutron spectrum. In the case of MOX fuels, ^{239}Pu has an even higher absorption cross-section. As a result, MOX-RG has the hardest spectrum due to the higher mass fraction of ^{239}Pu (Table 3).

Effect of soluble boric acid

Boric acid (H_3BO_3) is an important chemical compound to control excess reactivity. The presence of soluble boric acid in the moderator affects the group constants. As ^{10}B has a higher absorption cross-sections over the entire energy range, it has effects on both thermal and fast constants. In this study, the impact of boric acid (enriched to 19.9% with ^{10}B) on six distinct fuel types was examined across a concentration gradient of boric acid ranging from 900 ppm to 4700 ppm (900 ppm to

Table 5. Comparison of k_{eff} from SERPENT (reference) and COMSOL Multiphysics for different models of fuel assemblies with different fuels

Fuel	SERPENT (k_1) (Reference)	COMSOL Multiphysics (k_2)											
		Model 1		Model 2		Model 3		Model 4		Model 5		Model 6	
		k_2	$\lvert\Delta k\rvert/k_1$, pcm	k_2	$\lvert\Delta k\rvert/k_1$, pcm	k_2	$\lvert\Delta k\rvert/k_1$, pcm	k_2	$\lvert\Delta k\rvert/k_1$, pcm	k_2	$\lvert\Delta k\rvert/k_1$, pcm	k_2	$\lvert\Delta k\rvert/k_1$, pcm
UOX 3.0%	1.27432	1.26781	511	1.27405	21	1.27471	31	1.27413	15	1.27479	37	1.27600	132
UOX 4.0%	1.33018	1.32335	514	1.32989	22	1.33062	33	1.32993	19	1.33064	34	1.33188	128
UOX 4.45%	1.34823	1.34129	515	1.34795	21	1.34867	33	1.34796	20	1.34869	34	1.34996	129
Th	1.28709	1.28016	538	1.28634	58	1.28700	7	1.28493	167	1.28558	117	1.28670	30
MOX-RG	1.28819	1.28366	351	1.29197	294	1.29274	353	1.29204	299	1.29281	358	1.29326	394
MOX-WG	1.29821	1.28723	846	1.29197	480	1.29274	421	1.29204	475	1.29281	416	1.29326	381

Table 6. Two group constants for fuel zones of different cores for different fuels

Fuel	k_{eff}	$D_{(OSA)1}$	$D_{(OSA)2}$	Σ_f^1	Σ_f^2	υ_1	υ_2	Σ_a^1	Σ_a^2	$\Sigma_S^{1\to2}$	$\Sigma_S^{2\to1}$	β_{eff}
UOX 3%	1.2743	1.51	3.80E-01	2.58E-03	5.38E-02	2.55	2.44	9.38E-03	7.80E-02	1.72E-02	1.49E-03	7.01E-03
UOX 4%	1.3302	1.52	3.78E-01	3.11E-03	6.80E-02	2.54	2.44	1.00E-02	9.42E-02	1.67E-02	1.76E-03	6.97E-03
UOX 4.45%	1.3482	1.52	3.78E-01	3.34E-03	7.40E-02	2.53	2.44	1.03E-02	1.01E-01	1.65E-02	1.88E-03	6.99E-03
Th	1.2871	1.42	3.67E-01	3.66E-03	8.24E-02	2.52	2.44	1.20E-02	1.13E-01	1.57E-02	2.18E-03	6.98E-03
MOX-RG	1.2882	1.53	3.78E-01	3.34E-03	7.47E-02	2.53	2.44	1.03E-02	1.02E-01	1.56E-02	1.97E-03	5.47E-03
MOX-WG	1.2982	1.53	3.77E-01	3.38E-03	7.52E-02	2.53	2.44	1.04E-02	1.02E-01	1.63E-02	1.94E-03	5.36E-03

Table 7. Two group constants for radial reflectors of different cores for different fuels

Variants	$D_{(OSA)1}$	$D_{(OSA)2}$	$D_{(TRC)1}$	$D_{(TRC)2}$	Σ_a^1	Σ_a^2	$\Sigma_S^{1\to2}$	$\Sigma_S^{2\to1}$
UOX 3%	1.979	2.678E-01	6.973E-01	1.238E-01	3.701E-04	9.938E-03	4.197E-02	2.291E-04
UOX 4%	1.982	2.679E-01	6.988E-01	1.238E-01	3.685E-04	9.935E-03	4.168E-02	2.335E-04
UOX 4.45%	1.983	2.679E-01	6.994E-01	1.238E-01	3.678E-04	9.934E-03	4.156E-02	2.348E-04
Th	1.983	2.679E-01	6.991E-01	1.238E-01	3.686E-04	9.935E-03	4.166E-02	2.331E-04
MOX-RG	1.983	2.679E-01	6.991E-01	1.238E-01	3.686E-04	9.935E-03	4.166E-02	2.331E-04
MOX-WG	1.983	2.679E-01	6.991E-01	1.238E-01	3.686E-04	9.935E-03	4.166E-02	2.331E-04

Table 8. Two group constants for top and bottom reflectors of different cores for different fuels

Variants		$D_{(OSA)1}$	$D_{(OSA)2}$	$D_{(TRC)1}$	$D_{(TRC)2}$	Σ_a^1	Σ_a^2	$\Sigma_S^{1\to2}$	$\Sigma_S^{2\to1}$
UOX 3%	Reflector top part	2.032	2.662E-01	7.304E-01	1.238E-01	4.044E-04	9.986E-03	4.568E-02	1.641E-04
UOX 4%		2.032	2.662E-01	7.304E-01	1.238E-01	4.044E-04	9.986E-03	4.568E-02	1.641E-04
UOX 4.45%		2.032	2.662E-01	7.304E-01	1.238E-01	4.044E-04	9.986E-03	4.568E-02	1.641E-04
Th		2.010	2.664E-01	7.202E-01	1.238E-01	4.019E-04	9.982E-03	4.574E-02	1.658E-04
MOX-RG		2.068	2.665E-01	7.528E-01	1.238E-01	4.099E-04	9.977E-03	4.450E-02	1.806E-04
MOX-WG		2.073	2.664E-01	7.527E-01	1.238E-01	4.113E-04	9.979E-03	4.492E-02	1.717E-04
UOX 3%	Reflector bottom part	2.026	2.662E-01	7.272E-01	1.238E-01	4.048E-04	9.987E-03	4.582E-02	1.616E-04
UOX 4%		2.026	2.662E-01	7.272E-01	1.238E-01	4.048E-04	9.987E-03	4.582E-02	1.616E-04
UOX 4.45%		2.026	2.662E-01	7.272E-01	1.238E-01	4.048E-04	9.987E-03	4.582E-02	1.616E-04
Th		2.024	2.661E-01	7.262E-01	1.238E-01	4.038E-04	9.987E-03	4.583E-02	1.601E-04
MOX-RG		2.082	2.663E-01	7.594E-01	1.238E-01	4.088E-04	9.980E-03	4.430E-02	1.716E-04
MOX-WG		2.073	2.664E-01	7.554E-01	1.238E-01	4.118E-04	9.981E-03	4.485E-02	1.710E-04

Table 9. Two group constants for top and bottom Zircaloy layers of different cores for different fuels

Variants		$D_{(OSA)1}$	$D_{(OSA)2}$	$D_{(TRC)1}$	$D_{(TRC)2}$	Σ_a^1	Σ_a^2	$\Sigma_S^{1\to1}$	$\Sigma_S^{1\to2}$	$\Sigma_S^{2\to1}$	$\Sigma_S^{2\to2}$
UOX 3%	Top part Zircaloy layer	1.828	2.938E-01	1.628	2.770E-01	5.038E-04	9.443E-03	6.102E-01	3.573E-02	3.472E-04	1.763
UOX 4%		1.828	2.938E-01	1.628	2.770E-01	5.038E-04	9.443E-03	6.102E-01	3.573E-02	3.472E-04	1.763
UOX 4.45%		1.828	2.938E-01	1.628	2.770E-01	5.038E-04	9.443E-03	6.102E-01	3.573E-02	3.472E-04	1.763
Th		1.801	2.946E-01	1.655	2.829E-01	5.815E-04	1.145E-02	6.107E-01	3.466E-02	3.749E-04	1.748
MOX-RG		1.879	2.951E-01	1.735	2.833E-01	5.632E-04	1.142E-02	5.959E-01	3.083E-02	4.407E-04	1.747
MOX-WG		1.846	2.947E-01	1.702	2.831E-01	5.855E-04	1.144E-02	6.030E-01	3.418E-02	4.090E-04	1.748
UOX 3%	Bottom part Zircaloy layer	1.836	2.933E-01	1.836	2.933E-01	5.006E-04	9.450E-03	6.105E-01	3.573E-02	3.498E-04	1.765
UOX 4%		1.836	2.933E-01	1.836	2.933E-01	5.006E-04	9.450E-03	6.105E-01	3.573E-02	3.498E-04	1.765
UOX 4.45%		1.836	2.933E-01	1.836	2.933E-01	5.006E-04	9.450E-03	6.105E-01	3.573E-02	3.498E-04	1.765
Th		1.834	2.935E-01	1.834	2.935E-01	4.992E-04	9.443E-03	6.110E-01	3.516E-02	3.540E-04	1.764
MOX-RG		1.915	2.944E-01	1.916	2.944E-01	4.828E-04	9.426E-03	5.955E-01	3.140E-02	3.861E-04	1.763
MOX-WG		1.882	2.936E-01	1.882	2.936E-01	4.990E-04	9.445E-03	6.020E-01	3.464E-02	3.737E-04	1.765

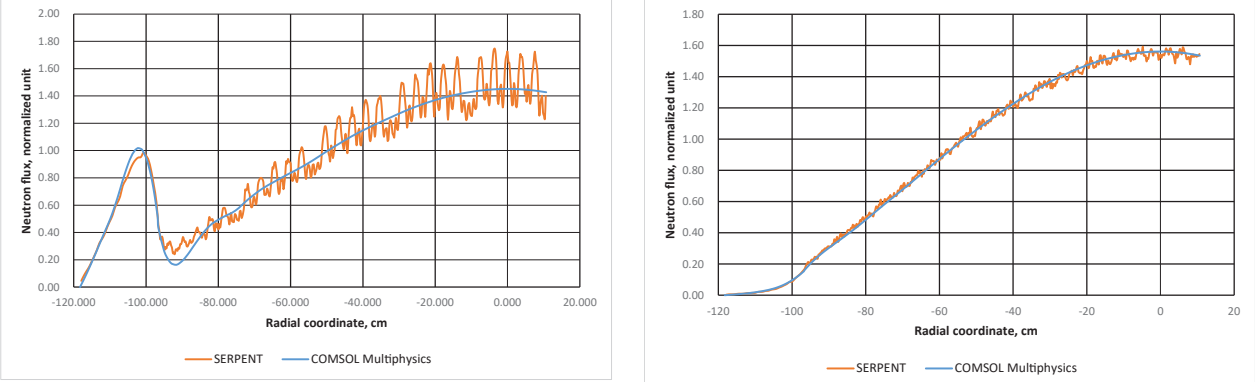

Figure 6. Radial Flux distribution of thermal and fast neutrons across the half of the active zone.

7500 ppm for MOX-RG) to show results in both supercritical and subcritical state. Comparison of the effectiveness of boric acid on different fuels is presented in Fig. 8. It can be observed that the effectiveness of boric acid to control reactivity is lower for MOX fuels, especially for MOX-RG. While for 4700 ppm of boric acid all the fuels show subcriticality ($k_{eff} < 1$), MOX-RG still remains in a supercritical state ($k_{eff} = 1.067$). For MOX-RG, the spectrum became more harder (Fig. 7), as Pu has comparatively higher absorption cross-sections than U and Th. Consequently, it reduces the effectiveness of boron regulation. So, additional analysis was undertaken with higher concentrations of boric acids in order to observe critical and subcritical states. For all of these concentrations, group constants were generated using TRC and OSA methods in SERPENT and those constants were used to determine k_{eff} from COMSOL Multiphysics. The comparisons of k_{eff} obtained from both programs are presented in Fig. 9. For all of the fuels, constants of the TRC method provide more accurate results except for MOX-RG. The maximum relative error of k_{eff} is less than 0.25% for the TRC method and around 0.45% for the OSA method. For MOX-RG, OSA method demonstrates higher accuracy. The maximum relative error is 0.86% for the OSA method and 1.06% for TRC method.

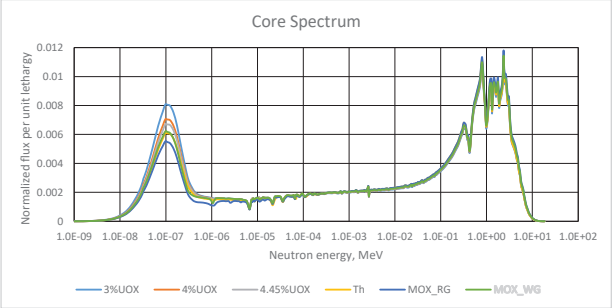

Figure 7. Spectrum of the core for different fuels.

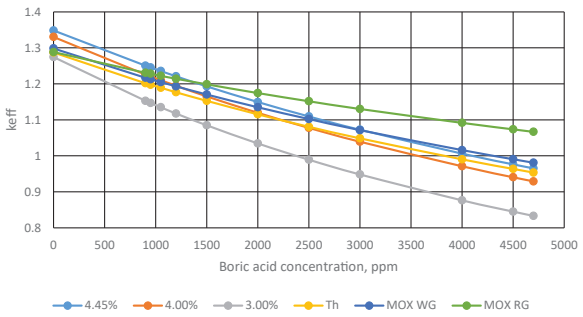

Figure 8. Dependence of k_{eff} on the concentration of boric acid for six distinct fuels.

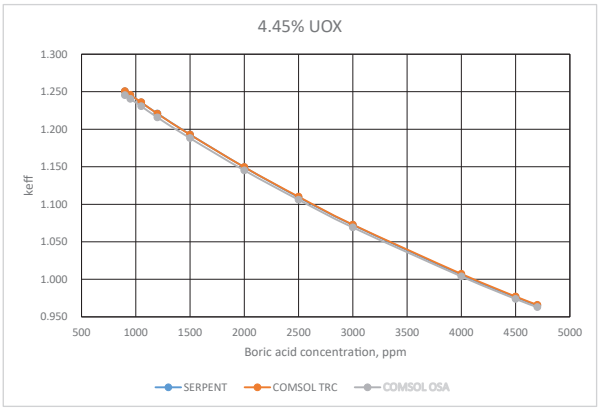

(a) UOX 4.45 wt.%

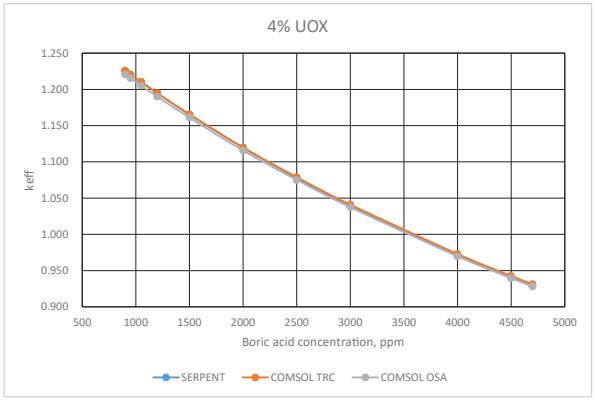

(b) UOX 4.0 wt.%

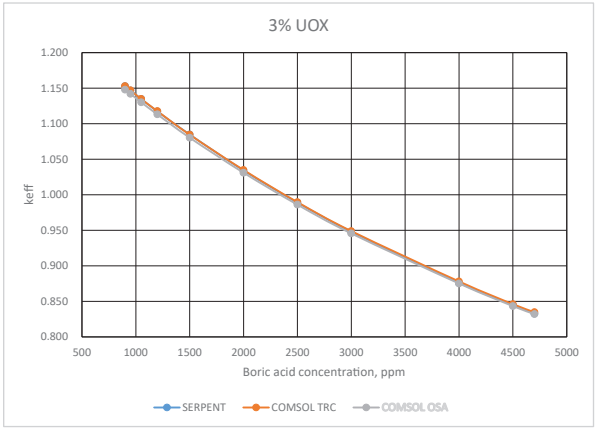

(c) UOX 3.0 wt.%

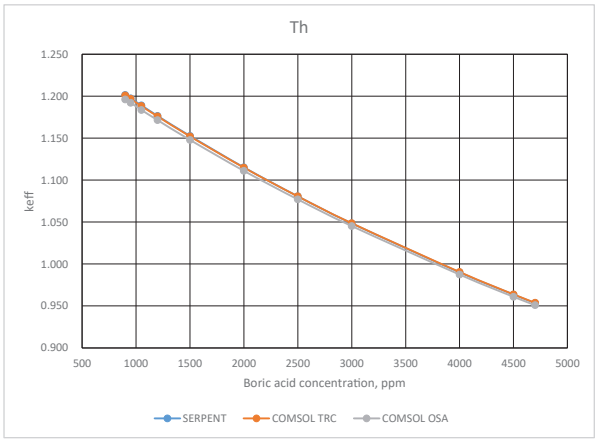

(d) Th

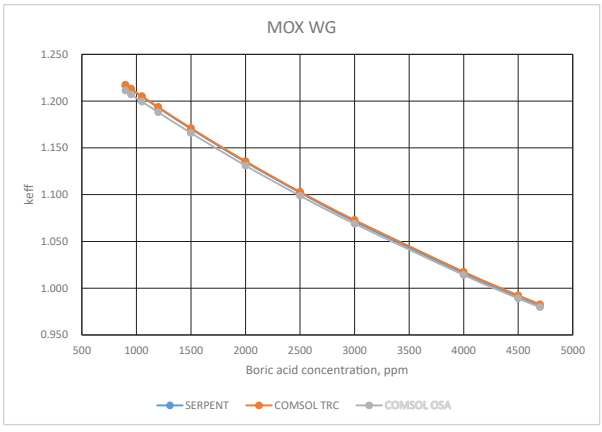

(e) MOX-WG

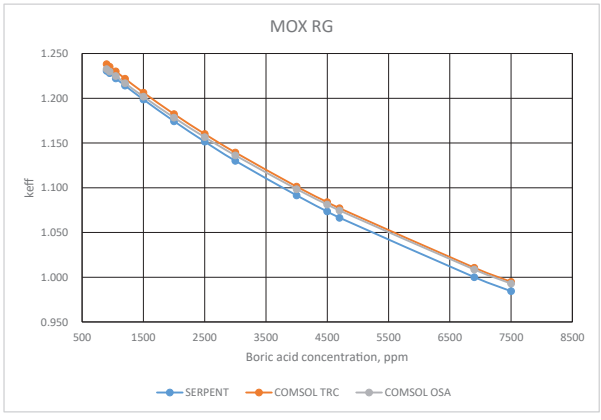

(f) MOX-RG

Figure 9. Comparison of k_{eff} dependence on boric acid concentration from SERPENT and COMSOL for different fuels. (**a**) UOX 4.45%, (**b**) UOX 4%, (**c**) UOX 3%, (**d**) Th, (**e**) MOX-WG, (**f**) MOX-RG.

Conclusion

The purpose of this study was to analyse the accuracy of diffusion coefficients and two-group macro constants for different material zones of the reactor using three separate methods: CMM, TRC and OSA by SERPENT for small modular reactors. Several sets of constants were evaluated to achieve higher accuracy in k_{eff} from SERPENT and COMSOL Multiphysics for six different fuels. For UOX with varying enrichment, Th, MOX-RG and MOX-WG fuels, models 4, 3, 2 and 6 produced more accurate results respectively. The smallest error margin is obtained for Th fuel, which is 0.007% while the best model for MOX-WG generates the highest error margin of 0.38% among all the fuels.

The effect of different fuels on the constants of non-fuel materials was also observed by OSA and TRC methods. It was found that fuel material changes the two-group constants of top and bottom reflectors and Zircaloy zones, but does not affect the radial reflector zone. Moreover, changing enrichment of UOX have no effect on constants of non-fuel materials.

A comparative analysis of the radial flux spectrum using both SERPENT and COMSOL demonstrated satisfactory accuracy, providing strong evidence for their suitability in this application. The agreement between the results from these two independent programs reinforces their reliability and credibility for this study.

Analysis of the energy spectrum revealed that the two-group diffusion equation was sufficient for thermal reactors since no resonance was observed in the thermal energy zones. 315 energy group were used to obtain the spectrum and it was also observed that for MOX-RG spectrum was the hardest and for 3% UOX it was the softest.

The effectiveness of soluble boric acid to control excess reactivity for six distinct fuels was also analyzed. Because of the hard neutron spectrum, boric acid has the least effect on excess reactivity for MOX-RG fuel, whereas its effect for 3% UOX fuel is the highest as due to the softest spectrum. While 4500 ppm of boric acid resulted in subcriticality for the other fuels, 6900 ppm of boric acid was required to manage the entire core excess reactivity for MOX-RG.

Change in the concentration of boric acid also affects constant generation. To analyse this effect, TRC and OSA methods were employed to generate diffusion coefficients and macro constants for various boric acid concentrations across all fuel types. The TRC method produced more accurate results for all the fuels with the maximum error margin of approximately 250 pcm, except for MOX-RG fuel. OSA method generated less error margin in reactivity for MOX-RG with the maximum value of 863 pcm. The two-group calculation method employed in this study can be utilized to build useful data libraries for detailed burnup calculations. Despite obtaining results with a sufficient degree of accuracy with only two group calculation without considering ADF, four or six-group calculation needs to be conducted in order to produce even more accurate results and effect of ADF can also be a topic of interest in the future work.

Acknowledgments

The work performed at NRNU MEPhI was supported by Ministry of science and higher education of Russian Federation under Project FSWU-2022-0016 and program "Priority 2030".

References

- Chadwick MB, Obložinský P, Herman M, Greene NM, McKnight RD, Smith DL, Young PG, MacFarlane RE, Hale GM, Frankle SC, Kahler AC, Kawano T, Little RC, Madland DG, Moller P, Mosteller RD, Page PR, Talou P, Trellue H, White MC, Wilson WB, Arcilla R, Dunford CL, Mughabghab SF, Pritychenko B, Rochman D, Sonzogni AA, Lubitz CR, Trumbull TH, Weinman JP, Brown DA, Cullen DE, Heinrichs DP, McNabb DP, Derrien H, Dunn ME, Larson NM, Leal LC, Carlson AD, Block RC, Briggs JB, Cheng ET, Huria HC, Zerkle ML, Kozier KS, Courcelle A, Pronyaev V, Van der Marck SC (2006) ENDF/B-VII. 0: next generation evaluated nuclear data library for nuclear science and technology. Nuclear Data Sheets 107(12): 2931–3060. https://doi.org/10.1016/j.nds.2006.11.001
- COMSOL (2008) COMSOL, Inc., COMSOL Multiphysics User's Guide, Version 3.5a, Burlington, MA.
- Fadaei AH (2011) Investigation of burnable poisons effects in reactor core design. Annals of Nuclear Energy 38(10): 2238–2246. https://doi.org/10.1016/j.anucene.2011.06.005
- Fejt F, Frybort J (2018) Analysis of a small-scale reactor core with PARCS/Serpent. Annals of Nuclear Energy 117: 25–31. https://doi.org/10.1016/j.anucene.2018.03.002
- Fejt F, Suk P, Frybort J, Rataj J (2022) Utilization of PARCS/Serpent in small-scale reactor–Multiplication factor, rod worth, and transient. Annals of Nuclear Energy 166: 108757. https://doi.org/10.1016/j.anucene.2021.108757
- Fridman E, Leppänen J (2011) On the use of the Serpent Monte Carlo code for few-group cross-sections generation. Annals of Nuclear Energy 38(6): 1399–1405. https://doi.org/10.1016/j.anucene.2011.01.032
- Galahom AA (2020) Investigate the possibility of burning weapon-grade plutonium using a concentric rods BS assembly of VVER-1200. Annals of Nuclear Energy 148: 107758. https://doi.org/10.1016/j.anucene.2020.107758
- Galahom AA (2021) Examine the possibility of increasing the plutonium incineration rate in the current operating pressurized water reactor. Progress in Nuclear Energy 142: 104026. https://doi.org/10.1016/j.pnucene.2021.104026
- Gürdal ŞO, Tombakoğlu M (2009) Two-group diffusion parameters for LWRs. In: Int. Conf. Nuclear Energy for New Europe NENE, 14–17.
- Herman BR, Forget B, Smith K, Aviles BN (2013) Improved diffusion coefficients generated from Monte Carlo codes. American

Nuclear Society, 555 North Kensington Avenue, La Grange Park, IL 60526 (United States).

- Ishraq MAR, Razu FM, Rohan HRK (2024a) Neutronic evaluation of diverse fuel configurations for the supercritical water reactor (SCWR) core. Nuclear Engineering and Design 423:113160. https://doi.org/10.1016/j.nucengdes.2024.113160
- Ishraq MAR, Rohan HRK, Kruglikov AE (2024b) Neutronic assessment and optimization of ACP-100 reactor core models to achieve unit multiplication and radial power peaking factor. Annals of Nuclear Energy 205: 110588. https://doi.org/10.1016/j.anucene.2024.110588
- Ishraq AR, Kruglikov AE, Rohan HRK (2024c) Strategic fuel management via implementation of a combined reload-reshuffle scheme in small modular reactors. Nuclear Engineering and Design 429: 113605. https://doi.org/10.1016/j.nucengdes.2024.113605
- Lamarsh JR, Baratta AJ (2001) Introduction to Nuclear Engineering (Vol. 3, 783 pp.). Upper Saddle River, NJ: Prentice hall.
- Lee JC (2020) Nuclear Reactor: Physics and Engineering. John Wiley & Sons. https://doi.org/10.1002/9781119582342
- Leppänen J (2013) Serpent–a continuous-energy Monte Carlo reactor physics burnup calculation code. VTT Technical Research Centre of Finland 4: 455.
- Leppänen J, Pusa M, Fridman E (2016) Overview of methodology for spatial homogenization in the Serpent 2 Monte Carlo code. Annals of Nuclear Energy 96: 126–136. https://doi.org/10.1016/j.anucene.2016.06.007
- Leppänen J, Pusa M, Viitanen T, Valtavirta V, Kaltiaisenaho T (2015) The Serpent Monte Carlo code: Status, development and applications in 2013. Annals of Nuclear Energy 82: 142–150. https://doi.org/10.1016/j.anucene.2014.08.024
- Liu Z, Smith K, Forget B, Ortensi J (2018) Cumulative migration method for computing rigorous diffusion coefficients and transport cross sections from Monte Carlo. Annals of Nuclear Energy 112: 507–516. https://doi.org/10.1016/j.anucene.2017.10.039
- Park HJ, Shim HJ, Joo HG, Kim CH (2012) Generation of few-group diffusion theory constants by Monte Carlo code McCARD. Nuclear Science and Engineering 172(1): 66–77. https://doi.org/10.13182/NSE11-22
- Shchurovskaya MV, Geraskin NI, Kruglikov AE (2020) Comparison of research reactor full-core diffusion calculations with few-group cross-sections generated using Serpent and MCU-PTR. Annals of Nuclear Energy 141: 107361. https://doi.org/10.1016/j.anucene.2020.107361
- Snoj L, Trkov A, Jaćimović R, Rogan P, Žerovnik G, Ravnik M (2011) Analysis of neutron flux distribution for the validation of computational methods for the optimization of research reactor utilization. Applied Radiation and Isotopes 69(1): 136–141. https://doi.org/10.1016/j.apradiso.2010.08.019
- Soppera N, Bossant M, Dupont E (2014) JANIS 4: an improved version of the NEA java-based nuclear data information system. Nuclear Data Sheets 120: 294–296. https://doi.org/10.1016/j.nds.2014.07.071
- Stacey WM (2018) Nuclear Reactor Physics. John Wiley & Sons. https://doi.org/10.1002/9783527812318
- Stammler RJ, Abbate MJ (1983) Methods of steady-state reactor physics in nuclear design.
- Ványi A, Hursin M, Czifrus S (2021) Investigation of Recently Introduced Diffusion Coefficient Generation Methods. In: International Conference Nuclear Energy for New Europe, 1–8.
- Vanyi AS, Hursin M, Czifrus S (2022) Analysis of diffusion coefficient correction methods applied for small-core, high-leakage reactors. Annals of Nuclear Energy 174: 109147. https://doi.org/10.1016/j.anucene.2022.109147
- Wan C, Bai J, Liu Y, Huang X, Wu H (2021) Method research and engineering application of the B10–abundance correction for PWR. Nuclear Engineering and Design 378: 111250. https://doi.org/10.1016/j.nucengdes.2021.111250
- Zheng SH, Vergnaud T, Nimal JC (1998) Neutron cross-section probability tables in TRIPOLI-3 Monte Carlo transport code. Nuclear science and Engineering 128(3): 321–328. https://doi.org/10.13182/NSE98-A1959
- Zhong F (2014) Safety features and licensing of CNNC-ACP100.